LAWRENCE
LIVERMORE
NATIONAL
LABORATORY

UCRL-JRNL-203237

Flat-field grating spectrometer for high-resolution soft x-ray and EUV measurements on an electron beam ion trap

P. Beiersdorfer, E. Magee, E. Träbert, H. Chen, J. K. Lepson, M. F. Gu, M. Schmidt

March 27, 2004

For submission to Review of Scientific Instruments

DISCLAIMER

Flat-field grating spectrometer for high-resolution soft x-ray and EUV measurements on an electron beam ion trap

P. Beiersdorfer[1], E. W. Magee[1], E. Träbert[1], H. Chen[1],

J. K. Lepson[2], M.-F. Gu[3], M. Schmidt[1*]

[1] *Lawrence Livermore National Laboratory, Livermore, CA 94550, USA*

[2] *University of California, Berkeley, CA 94720, USA*

[3] *Stanford University, Palo Alto, CA 94305, USA*

Abstract

A R = 44.3 m grazing-incidence grating spectrometer has been implemented on the Livermore electron beam ion traps for high-resolution measurements in the soft x-ray and extreme ultraviolet region spanning from below 10 Å up to 50 Å. The instrument uses a grating with variable line spacing (about 2400 ℓ/mm) for a flat field of view. Spectra are recorded with a back-illuminated charge-coupled device detector. The new instrument greatly improves upon the resolution achieved with existing grating spectrometers and complements crystal spectrometers at the shorter wavelengths both in terms of wavelength coverage and polarization independent reflectivity response.

I. INTRODUCTION

Spectra obtained with the space-based Chandra and XMM-Newton X-ray Observatories have shown the tremendous utility of emission lines in the soft x-ray and extreme ultraviolet

*Permanent address: Technische Universität Dresden, Germany

(EUV) wavelength region as diagnostics of high temperature astrophysical plasmas [1–4]. Emphasis of these measurements is on the iron L-shell spectrum situated between about 10 and 17 Å, as well as K-shell spectra of magnesium, neon, oxygen, nitrogen, and carbon in the 8 to 45 Å region. The resolving power of these instruments is typically several hundred [5–7]. However, the resolving power achieved with Chandra's High Energy Transmission Grating Spectrometer (HETGS) exceeds $\lambda/\Delta\lambda = 1000$ near 15 Å.

Laboratory measurements, typically carried out on electron beam ion traps or tokamaks, are needed to aid the interpretation of the astrophysical spectra [8], and such measurements require spectrometers with equal or better resolving powers than those of the space-based x-ray observatories. Grating spectrometers have been implemented only recently on electron beam ion traps [9–11]. However, these instruments have a resolution less than that of the HETGS aboard Chandra. At the University of California Lawrence Livermore National Laboratory these instruments have used an R = 5.65 m or 15.9 m grating and achieve resolving powers of 300–400 in slitless operation (somewhat greater in higher orders) [9,10]. The resolution for lines with wavelength below about 20 Å was too poor to compete with crystal spectrometers. As a result, iron L-shell spectra near 15 Å were measured with crystal spectrometers that have had typical resolving power of 500 [12,13]. A 2 m grazing-incidence spectrometer based on a design by Schwob and Fraenkel was installed at the Berlin electron beam ion trap, providing line widths of 0.2 Å when employing an 18 μm entrance slit and thus resolving powers in the 50–100 Å region similar to those of the Livermore instruments [11]. The short-wavelength performance of the Berlin instrument has not yet been reported to our knowledge, but is expected to be similar to that of instruments installed at various tokamak facilities [14], i.e., $\lambda/\Delta\lambda \approx 140$ at 15 Å, provided a narrower slit (10 μm) and a 2400 ℓ/mm grating are employed.

In order to produce spectra from laboratory plasmas with equal or better resolution than the astrophysical spectra we have constructed an R = 44.3 m, flat-field grating spectrometer for use on the University of California Lawrence Livermore National Laboratory electron beam ion traps. This instrument was installed on the EBIT-I electron beam ion trap and

has rapidly become the instrument of choice for soft x-ray and EUV spectroscopy at our facility.

II. INSTRUMENT DESIGN AND PERFORMANCE

A schematic of the spectrometer implemented on EBIT-I is shown in Fig. 1. The spectrometer employs a ruled diffraction grating with variable line spacing and an angle of incidence of about 2° similar to that used in the previously described EUV spectrometers in use at the Livermore electron beam ion traps [9,10,15]. The average spacing is 2400 ℓ/mm. The main diffference is the radius of curvature of 44.3 m, which is three to eight times larger than in the earlier instruments. The variable spacing provides a nearly flat image field, and we use a thinned, back-illuminated charge-coupled device (CCD) detector with 1340 × 1300 pixels of 20 μm × 20 μm area each pixel for readout [16].

The 50–60 μm diameter electron beam [17] serves as an quasi entrance slit for many of the spectrometers on the Livermore electron beam ion traps [18,19], and we have employed a similar configuration for the new spectrometer. The EBIT-I electron beam is located close to, but not exactly at, the design entrance slit location of the new spectrometer. A typical line width of four pixels is obtained. This corresponds to 80 μm, which is about a 30 % larger than the width expected, if the electron beam was fully in focus.

The entire spectrometer is affixed to a passive vibration system in order to minimize mechanical vibration influences. The detector arm is then floated on a compressed air bearing. This combination helps reduce line broadening effects of vibrations and allows us to easily set the detector to different parts of the spectral region of interest. The detector to the grating distance can be adjusted by a micro-step motor drive to bring the detector in focus when the wavelength range is changed. The CCD detector may also be moved by a micro step motor in order to scan for additional spectra. The vacuum in the spectrometer, to be compatible with that of the electron beam ion trap, is maintained in the 10^{-8} torr range by two turbo pumps and by cooling the CCD camera with liquid nitrogen.

Figure 2 compares the spectrum composed of $n = 3 \rightarrow n = 2$ transitions in Ar^{8+}–Ar^{10+} obtained with the new spectrometer near 35 Å to that obtained with the 15.9 m grazing incidence grating spectrometer used earlier [20] on EBIT-I. A uniform background was subtracted in both cases. In addition, events caused by cosmic rays were filtered out from each two-dimensional CCD image before summing channels perpendicular to the dispersion direction. For image manipulation we used IPLab software [21] running on a G3 Macintosh computer, which is also used for data acquisition and camera control. The increase in resolving power of the new instrument is readily apparent. The resolving power of the new instrument in this wavelength region is about 1200 (observed line width 0.029 Å); that of the older spectrometer, which used the 15.9 m grating, is 400 (observed line width 0.09 Å). The increase roughly scales with the increase in the radius of curvature of the two gratings. The increased resolving power, however, comes at the expense of single-setting spectral coverage: 33–43 Å with the new spectrometer versus 10–55 Å with the older spectrometer.

The new spectrometer also achieves excellent resolving power and reflectivity response for soft x rays. In Figure 3 we show a spectrum of the neonlike Fe XVII lines centered near 16 Å. The resolving power is about 600, which equals that achieved in this wavelength region on our device with flat-crystal spectrometers [12,13] and is comparable to the resolution achieved with Chandra's Low Energy Transmission Grating Spectrometer in orbit (e.g., [22]). The figure also shows the emission of the Rydberg series of hydrogen- and heliumlike oxygen.

The relative intensity of the Rydberg lines can be used to infer the response of the new spectrometer. The ratios of the Rydberg lines, such as O VIII Lyman-α to Lyman-β or Lyman-γ are theoretically known to within about 10 % in the high-energy limit and have also been measured [8]. We measured these ratios at high electron beam energy ($\geq$ 2 keV) for the strongest Rydberg lines of O VIII, F VIII, F IX, Ne IX, and Ne X and compared them to the results from distorted-wave calculations. The agreement of the measured intensity ratio with that from theory is within the estimated accuracy of the calculation for all line pairs, as shown in Fig. 4. From this agreement we infer that the instrumental response is

flat in the region between 11 and 19 Å.

The spectral range observed in the soft x-ray range with the new spectrometer is wider than that observed with our crystal spectrometers. Early measurements of the Fe XVII spectrum from 13.5 to 17.5 Å on the Livermore EBIT-II device took three spectrometer settings [12] because of limitations in the crystal length. This was improved later with a two-crystal spectrometer [13]. This instrument could record the $n = 3 \rightarrow n = 2$ Fe XVII spectrum from 13 to 18 Å in one measurement but requiring two separate detectors. The new grating spectrometer observes 13 to 19 Å in a single setting.

In Fig. 5 we show a measurement of the heliumlike Mg^{10+} K-shell lines near 9 Å. Although the resolving power is considerably less than what can be achieved with a crystal spectrometer in this wavelength region [23], it is still about 165 (0.06 Å line width). Grating spectrometers can be used in conjunction with crystal spectrometers to measure the linear polarization of the observed x-ray lines [10]. The reason is that grazing incidence spectrometers reflect both polarization equally well, while crystal spectrometers operating near the Brewster angle at 45° select only one of the two components [24,25]. The observation of the heliumlike Mg^{10+} K-shell demonstrates that the new spectrometer will allow determinations of line polarization well into the soft x-ray regime.

III. OUTLOOK

There are still many areas of operation yet to be explored by the new LLNL grating spectrometer. Replacing the time-integrating CCD detector (50 second read-out time) with a microchannel-plate detector will provide time-resolved detection of individual photons. With this setup we will be able to use the spectrometer for radiative lifetimes measurements using the magnetic trapping mode on an electron beam ion trap [26–28] as well as for measurements of the variation of the line emission with electron beam parameters [29].

It is also planned to implement the new spectrometer on the Livermore SuperEBIT electron beam ion trap where it will be used for wavelength measurements of the $2p_{1/2} \rightarrow 2s_{1/2}$

transition in lithiumlike U^{89+}. This transition is strongly affected by quantum electrodynamics. A first use of the spectrometer was recently reported [30] for precision wavelength measurements of the K-shell resonance lines in lithiumlike O^{5+} and berylliumlike O^{4+} needed for analyzing absorption spectra of warm absorbers outside active galactic nuclei observed with the Chandra X-ray Observatory. These measurements attained accuracies as high as 70 ppm, proving the use of the new instrument for precision wavelength determinations.

IV. ACKNOWLEDGEMENT

This work was performed under the auspices of the U.S. DOE by the University of California Lawrence Livermore National Laboratory under contract W-7405-Eng-48 and supported by NASA's Astronomy and Physics Research and Analysis Program under work order S-06553-G.

REFERENCES

[1] A. C. Brinkman *et al.*, Astrophys. J. (Lett.) **530**, L111 (2000).

[2] C. R. Canizares *et al.*, Astrophys. J. **539**, L41 (2000).

[3] F. Paerels *et al.*, Astrophys. J. (Lett.) **533**, L135 (2000).

[4] A. C. Brinkman *et al.*, Astron. Astrophys. **365**, L324 (2001).

[5] T. H. Markert *et al.*, Proc. SPIE **2280**, 168 (1994).

[6] A. C. Brinkman *et al.*, Proc. SPIE **3113**, 181 (1997).

[7] J. W. den Herder *et al.*, Astron. Astrophys. **365**, L7 (2001).

[8] P. Beiersdorfer, Ann. Rev. Astron. Astrophys. **412**, 343 (2003).

[9] P. Beiersdorfer *et al.*, Rev. Sci. Instrum. **70**, 276 (1999).

[10] S. B. Utter *et al.*, Rev. Sci. Instrum. **70**, 284 (1999).

[11] R. Radtke *et al.*, Phys. Rev. A **64**, 012720 (2001).

[12] P. Beiersdorfer and B. J. Wargelin, Rev. Sci. Instrum. **65**, 13 (1994).

[13] G. V. Brown, P. Beiersdorfer, and K. Widmann, Rev. Sci. Instrum. **70**, 280 (1999).

[14] J. L. Schwob, A. W. Wouters, S. Suckewer, and M. Finkenthal, Rev. Sci. Instrum. **58**, 1601 (1987).

[15] T. Kita, T. Harada, N. Nakano, and H. Kuroda, Appl. Opt. **22**, 512 (1983).

[16] Roper Scientific, 3660 Quakerbridge Road, Trenton, NJ 08619, .

[17] S. B. Utter, P. Beiersdorfer, J. R. Crespo López-Urrutia, and K. Widmann, Nucl. Instrum. Methods **A 428**, 276 (1999).

[18] P. Beiersdorfer, R. E. Marrs, J. R. Henderson, D. A. Knapp, M. A. Levine, D. B. Platt, M. B. Schneider, D. A. Vogel, and K. L. Wong, Rev. Sci. Instrum. **61**, 2338 (1990).

[19] J. R. Crespo López-Urrutia, P. Beiersdorfer, K. Widmann, and V. Decaux, Can. J. Phys. **80**, 1687 (2002).

[20] J. K. Lepson, P. Beiersdorfer, E. Behar, and S. M. Kahn, Astrophys. J. **590**, 604 (2003).

[21] Scanalytics, 8550 Lee Highway Suite 400, Fairfax, VA 22031, .

[22] T. R. Ayres *et al.*, Astrophys. J. **549**, 554 (2001).

[23] P. Beiersdorfer *et al.*, Rev. Sci. Instrum. **68**, 1077 (1997).

[24] P. Beiersdorfer *et al.*, Rev. Sci. Instrum. **68**, 1073 (1997).

[25] A. S. Shlyaptseva, R. C. Mancini, P. Neill, and P. Beiersdorfer, Rev. Sci. Instrum. **68**, 1095 (1997).

[26] P. Beiersdorfer, L. Schweikhard, J. Crespo López-Urrutia, and K. Widmann, Rev. Sci. Instrum. **67**, 3818 (1996).

[27] E. Träbert, Can. J. Phys. **80**, 1481 (2002).

[28] E. Träbert and P. Beiersdorfer, Rev. Sci. Instrum. **74**, 2127 (2003).

[29] P. Beiersdorfer *et al.*, Rev. Sci. Instrum. **72**, 508 (2001).

[30] M. Schmidt *et al.*, Astrophys. J. .

[31] M.-F. Gu, Astrophys. J. **582**, 1241 (2003).

[32] R. K. Smith and N. S. Brickhouse, RevMexAA **9**, 134 (2000).

FIGURES

FIG. 1. Schematic of the R = 44.3 m grating spectrometer on the EBIT-I electron beam ion trap.

FIG. 2. L-shell emission of Ar IX,, Ar X, and Ar XI observed on EBIT-I with (a) the new R= 44.3 m grazing incidence spectrometer and (b) the older R = 15.9 m spectrometer.

FIG. 3. Spectra of (a) $n = 3 \rightarrow n = 2$ transitions in Fe^{16+} and (b) $np \rightarrow 1s$ transitions in heliumlike and hydrogenlike oxygen. The Fe XVII lines are labeled $3C$, $3D$, $3E$, $3F$, $3G$, and $M2$, denoting the transitions from upper levels $(2p^5_{1/2}3d_{3/2})_{J=1}$, $(2p^5_{3/2}3d_{5/2})_{J=1}$, $(2p^5_{3/2}3d_{3/2})_{J=1}$, $(2p^5_{1/2}3s_{1/2})_{J=1}$, $(2p^5_{3/2}3s_{1/2})_{J=1}$, and $(2p^5_{3/2}3s_{1/2})_{J=2}$, respectively, to the $(2p^6)_{J=0}$ closed-shell ground state. Lyα through Lyδ denotes the $np \rightarrow 1s$ transitions with n =2, 3, 4, and 5, respectively, in hydrogenlike O VIII. Heβ through Heζ denotes the $1snp \rightarrow 1s^2$ transitions with n =3, 4, 5, and 6, respectively, in heliumlike O VII.

FIG. 4. Comparison of the measured and calculated intensity ratios of various hydrogenlike and heliumlike Rydberg lines. Top: intensity ratio of the Lyβ to Lyα lines in hydrogenlike O^{7+} compared to calculations using the Flexible Atomic Code (FAC) [31] and the Astrophysical Plasma Emission Code (APEC) [32]. The average of the six measurements is indicated by the gray band. Bottom: Deviation of the measured line ratios from those calculated with FAC. Different symbols denote line ratios in Ne IX (solid squares), F IX (open squares), F VIII (solid circles), and O VIII (open circles).

FIG. 5. K-shell Spectrum of heliumlike Mg^{10+}. w, y, and z denote the transitions from upper levels $1s2p\ ^1P_1$, $1s2p\ ^3P_1$, and $1s2s\ ^3S_1$ to the heliumlike $1s^2\ ^1S_0$ ground state. q denotes the $1s2s2p\ ^2P_{3/2} \rightarrow 1s^2 2s\ ^2S_{1/2}$ transition in lithiumlike Mg^{9+}.

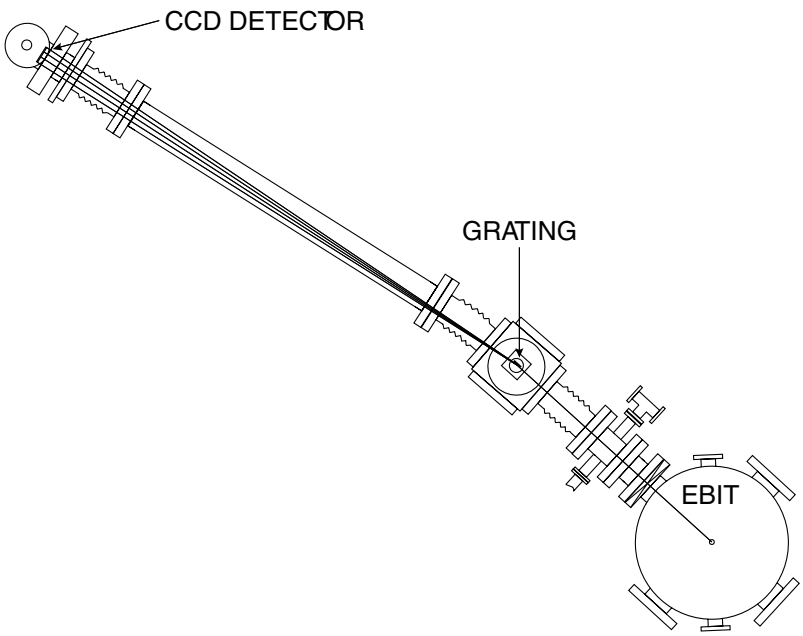

Fig. 1

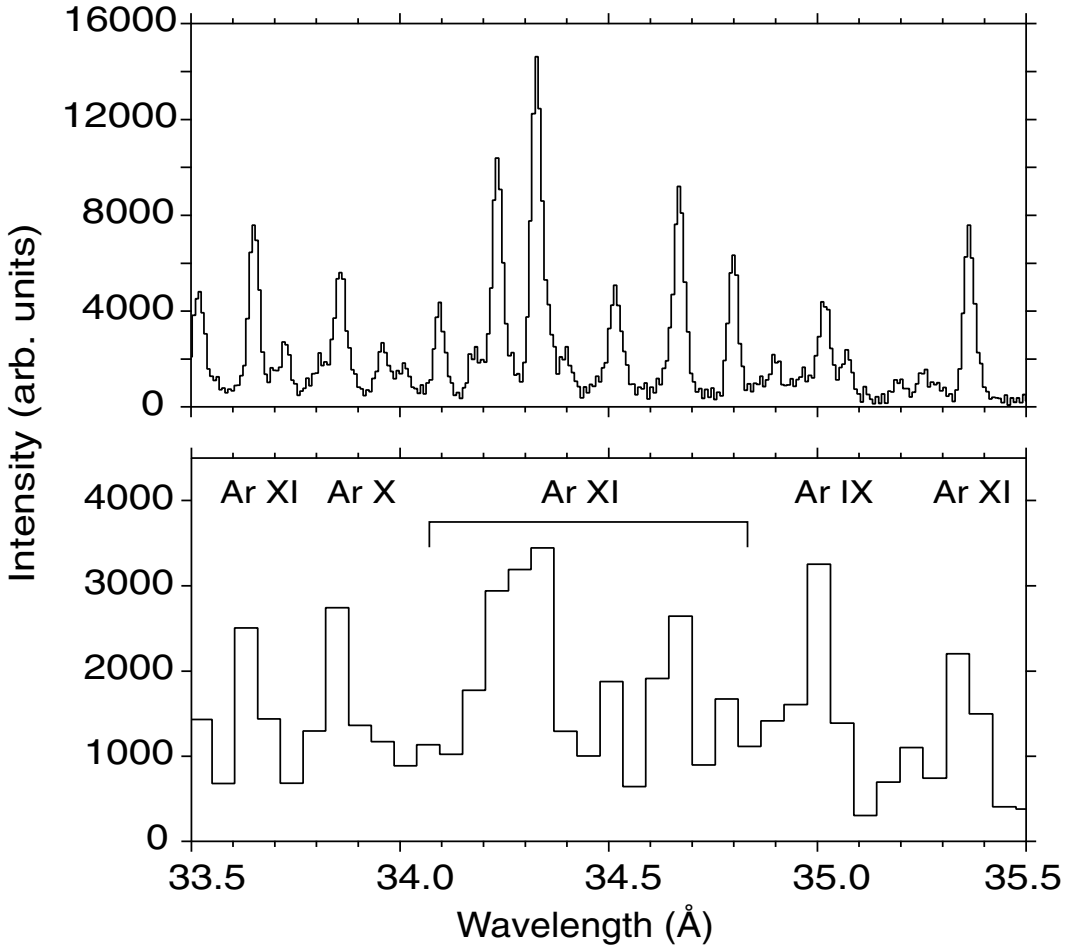
16000
12000
8000
4000
0
Intensity (arb. units)
4000
3000
2000
1000
0
Ar XI
Ar X
Ar XI
Ar IX
Ar XI
33.5
34.0
34.5
35.0
35.5
Wavelength (Å)

Fig. 2

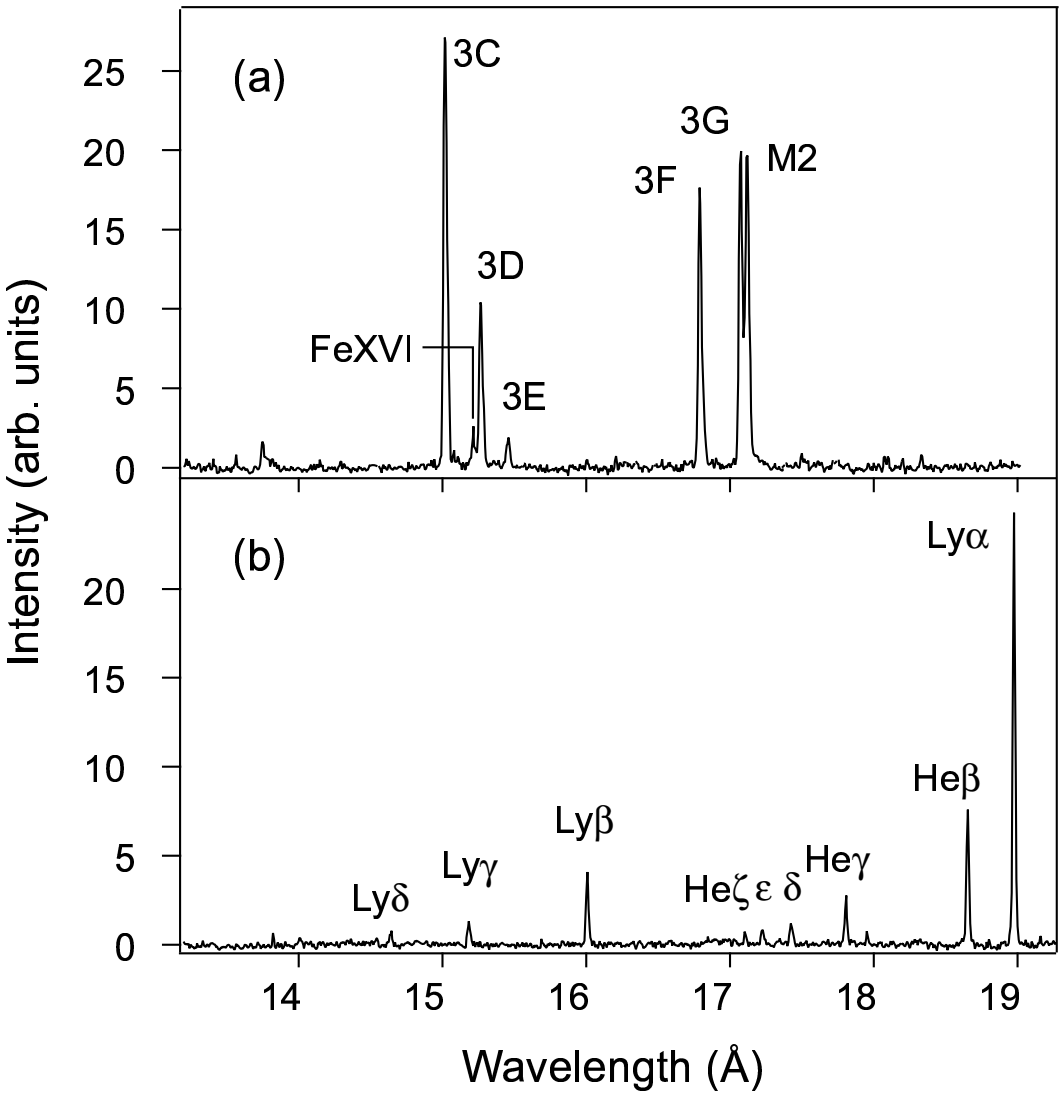
(a)
3C
3G
3F
M2
3D
FeXVI
3E
(b)
Lyα
Heβ
Lyβ
Lyγ
Heγ
Lyδ
Heζ ε δ
Intensity (arb. units)
Wavelength (Å)

Fig. 3

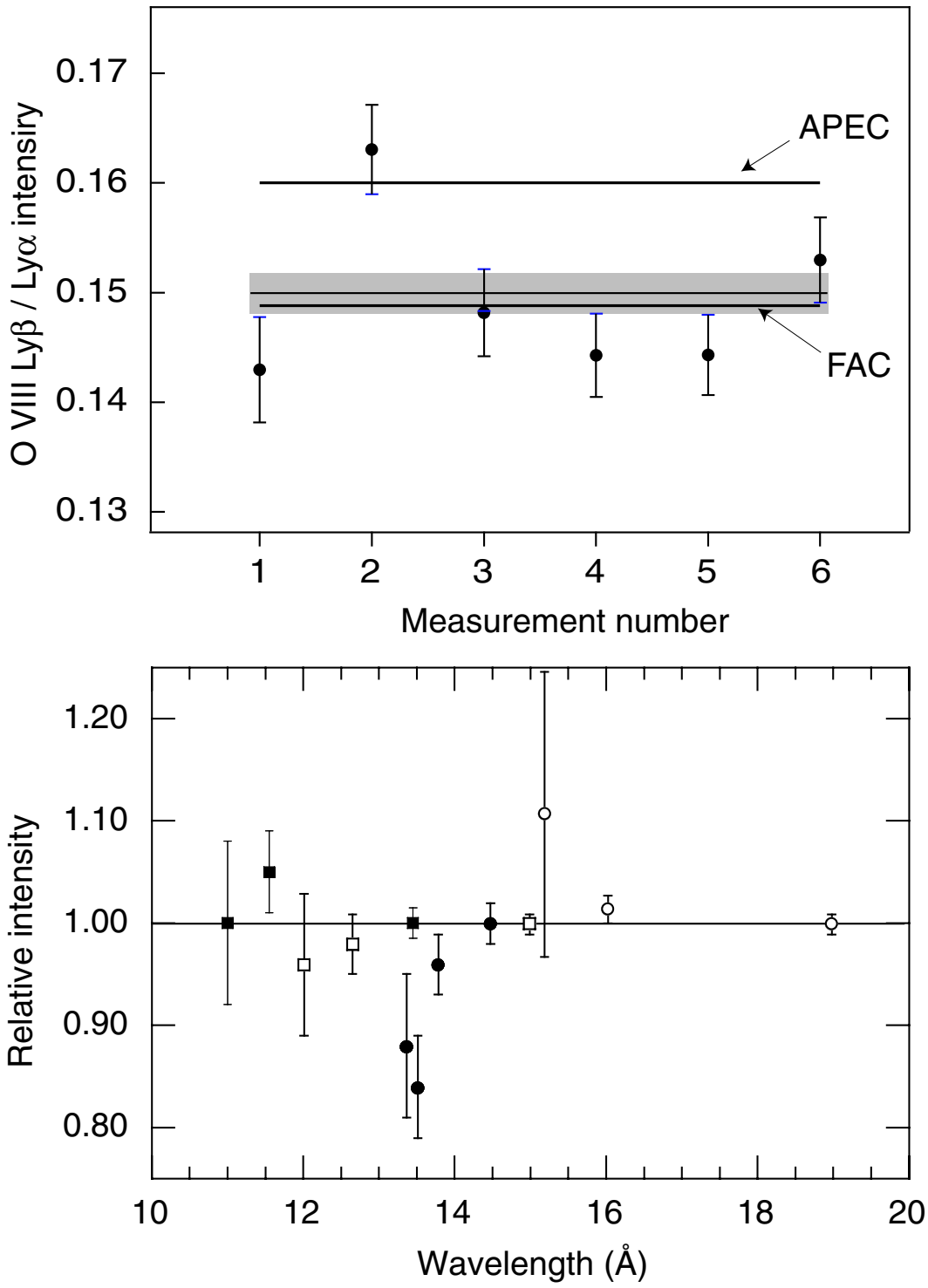
0.17
0.16
0.15
0.14
0.13
O VIII Lyβ / Lyα intensiry
APEC
FAC
1
2
3
4
5
6
Measurement number
1.20
1.10
1.00
0.90
0.80
Relative intensity
10
12
14
16
18
20
Wavelength (Å)

Fig. 4

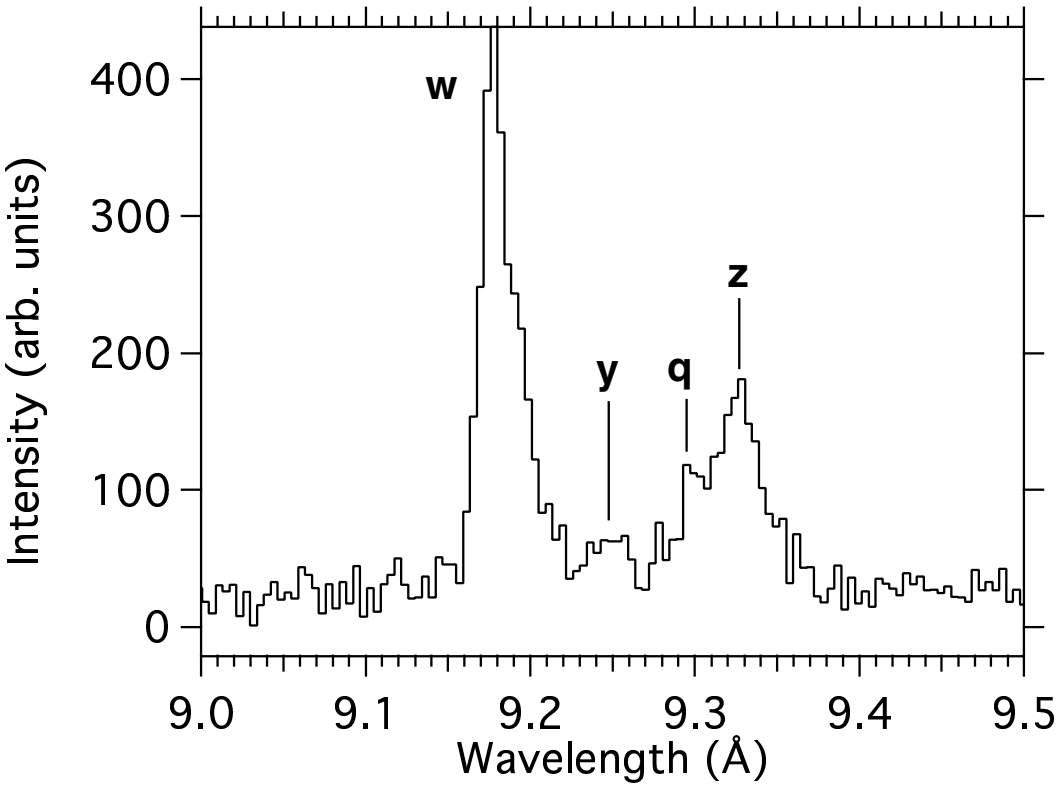
w
y
q
z
400
300
200
100
0
Intensity (arb. units)
9.0
9.1
9.2
9.3
9.4
9.5
Wavelength (Å)

Fig. 5

University of California
Lawrence Livermore National Laboratory
Technical Information Department
Livermore, CA 94551